Available online at www.sciencedirect.com

ScienceDirect

IFAC PapersOnline CONFERENCE PAPER ARCHIVE

IFAC PapersOnLine 55-37 (2022) 694–699

Designing Traffic Management Strategies for a Heterogeneous Traffic Network

Pouria Karimi Shahri * **Baisravan HomChaudhuri** ** **Azad Ghaffari** *** **Amir H. Ghasemi** *

* *Department of Mechanical Engineering, the University of North Carolina at Charlotte, Charlotte, NC, 28223 (e-mail: Pkarimis@uncc.edu, ah.ghasemi@uncc.edu*

** *Baisravan Homechduri is with Faculty of the Department of Mechanical Engineering, Illinois Institute of Technology, Chicago, IL, USA (e-mail: bhomchaudhuri@iit.edu)*

*** *Department of Mechanical Engineering, Wayne State University, Detroit, MI, USA (e-mail: aghaffari@wayne.edu)*

Abstract: This paper focuses on modeling and controlling a non-signalized heterogeneous traffic network consisting of Human-Driven Vehicles (HDVs) and Autonomous Vehicles (AVs) at a macroscopic level. To describe the traffic network's behavior, we introduce an extended heterogeneous METANET model wherein each vehicle class's density and velocity dynamics are described. To develop traffic control policies, we propose a two-level control structure. At the higher level, a decentralized Extremum-Seeking (ES) control approach is designed to determine an optimal density of human and autonomous vehicles so that the average flow within the cell is maximized. At the lower level, a filtered feedback linearization control approach is designed to determine the velocity of autonomous and human-driven vehicles such that the density of each type of vehicle reaches the values set by the upper-level macroscopic controller. Numerical simulation demonstrates the effectiveness of the proposed approach in managing the traffic flow of a heterogeneous system.

Copyright © 2022 The Authors. This is an open access article under the CC BY-NC-ND license (https://creativecommons.org/licenses/by-nc-nd/4.0/)

Keywords: Heterogeneous Traffic Network, Adaptive Extremum Seeking Control, Filtered Feedback Linearization Control, Autonomous Vehicles

1 INTRODUCTION

Traffic jams cost US $87 billion in 2018 (Cookson and Pishue (2017)). Different control strategies with different traffic flow models have been developed to manage traffic networks (Lazar et al. (2018)). Among these efforts, connected automated vehicle (CAV) technologies have received increasing attention recently (Lazar et al. (2018)). Recent studies have shown the positive impacts of CAVs technology on fuel consumption, reduced travel time, and improved safety (Ross and Guhathakurta (2017); Ye and Yamamoto (2018)). However, for practical purposes, (i) no traffic network in the near future will consist entirely of automated vehicles, and (ii) vehicles (even automated ones, but especially the human-driven ones) will never behave entirely homogeneously. Until then, there exists significant uncertainty in the performance of mixed CAV and human-driven traffic environments (Sharon and Stone (2017); Wang et al. (2019); Zheng et al. (2020)). Therefore, it is essential to develop control strategies that take into account the uncertainty associated with the heterogeneity in the traffic network and understand the extent to which these strategies improve the performance of the network.

To manage the congestion in a heterogeneous traffic network, a two-level control structure is proposed. In the higher level, a decentralized ES control approach is developed. ES is a real-time control technique that optimize the steady-state behaviour of an unknown system which is done by estimating the gradients of the input-output mapping. (DeHaan and Guay (2005), Shahri et al. (2020)) At the lower level, we employed Filtered Feedback linearization (FFL) to determine the suggested velocity for each class of vehicles so that the desired density determined in the upper level can be achieved.

FFL is a high-parameter-stabilizing controlling approach that helps to follow the reference commands and also rejects the unknown disturbance in MIMO (Multi-Input-Multi-Output) nonlinear dynamic systems where the equilibrium of the zero dynamics is locally asymptotically stable (Hoagg and Seigler (2013)). Mathematically, FFL is equivalent to passing the classic feedback linearization controller's output to a low-pass filter. Nevertheless, unlike the classic feedback linearization control approach, the controller only needs a very limited information from the dynamic model, specifically, knowledge of the the dynamic-inversion matrix and also the vector relative degree. (Hoagg and Seigler (2015), Shahri and Ghasemi (2022))

The outline of this paper is as follows. Sections 2 presents the model of a heterogeneous traffic network using heterogeneous METANET model. Section 3 presents the basics

⋆

2405-8963 Copyright © 2022 The Authors. This is an open access article under the CC BY-NC-ND license.
Peer review under responsibility of International Federation of Automatic Control.
10.1016/j.ifacol.2022.11.263

of a two-level controller to maximize the mobility of the traffic network. Section 4 presents numerical results, and section 5 is the conclusion where we also discuss our future plans.

2 Macroscopic Dynamics of a Heterogeneous Traffic Network

Consider a non-signalized heterogeneous traffic network wherein the road is shared between the human-driven vehicles and autonomous vehicles. The road can be discretized into multiple cells. We characterize cell $i \in \{1, 2, \cdots, n\}$ by its length ℓ_i, density of human-driven and autonomous vehicles $(k_{i,\mathrm{H}}, k_{i,\mathrm{A}})$, space mean speed of each class $(v_{i,\mathrm{H}}, v_{i,\mathrm{A}})$, and the total outflow rate q_i. To determine the fundamental relation between the average flow(Q_i), density(k_i) and space mean speed v_i, we adopt a heterogeneous METANET model (Liu et al. (2014)).

2.1 Heterogeneous METANET Model

The heterogeneous METANET model is an extension of the well-known METANET model (Papageorgiou (1983)). In this model, in cell $i \in \{1, \cdots, n\}$, for each class of vehicles, two set of fundamental diagrams is defined that describe the macroscopic behavior of autonomous and human-driven vehicles in a homogeneous (fully autonomous or fully human-driven) traffic network. In the two set of fundamental diagrams, $(v_{\mathrm{f,A}} \geq v_{\mathrm{f,H}})$, critical density $(k_{\mathrm{c,A}} \geq k_{\mathrm{c,H}})$, capacity $(C_{\mathrm{A}} \geq C_{\mathrm{H}})$ and jam density $(k_{\mathrm{J,A}} \geq k_{\mathrm{J,H}})$ is assumed for autonomous vehicles with respect to human-driven vehicles. In the heterogeneous METANET model, based on the fundamental diagram properties of each class of vehicles and their densities within the cell, the road is divided into two sections and it is assumed that each type of vehicle limit itself within the allocated space of the road (Logghe (2003)). Therefore, the road fractions for various types of vehicles are positive $(\alpha_{i,\mathrm{A}} \geq 0, \alpha_{i,\mathrm{H}} \geq 0)$, and the sum of all fractions is $\alpha_{i,\mathrm{A}} + \alpha_{i,\mathrm{H}} = 1$.

To determine α_{A} and α_{H}, various approaches have been proposed.(Benzoni-Gavage and Colombo (2003), Chanut and Buisson (2003))

In this paper, according to different densities and their relative behavior in the traffic network, three traffic phases are distinguished (Liu et al. (2014)): free-flow, semi-congested, congested. These phases are defined in below. For all of these phases, we consider that each type of vehicle occupies the road optimally and never occupies more space than is necessary.

Free-Flow Phase: Both human-driven and autonomous vehicles drive at their free-flow velocity. To this end, in the free-flow phase, it is assumed that density of HDVs and AVs in their optimal assigned space is less than or equal to the critical density of each vehicle class. The optimal space fractions of each vehicle class in the free-flow phase are:

$$\begin{aligned} \alpha_{ff,i,\mathrm{H}} &= \frac{k_{i,\mathrm{H}} k_{c,\mathrm{A}}}{k_{i,\mathrm{H}} k_{c,\mathrm{A}} + k_{i,\mathrm{A}} k_{c,\mathrm{H}}} \\ \alpha_{ff,i,\mathrm{A}} &= \frac{k_{i,\mathrm{A}} k_{c,\mathrm{H}}}{k_{i,\mathrm{A}} k_{c,\mathrm{H}} + k_{i,\mathrm{H}} k_{c,\mathrm{A}}} \end{aligned} \tag{1}$$

where $k_{\mathrm{c,H}}$ and $k_{\mathrm{c,A}}$ are representing the critical density of HDVs and AVs respectively.

Semi-Congested Phase: The vehicle class with a smaller free-flow velocity (i.e., HDVs) drive at the free-flow velocity but the other vehicle class with a larger free-flow velocity (i.e., AVs) experience a congestion and drive at a speed lower than its free-flow velocity. The important point in the semi-congested phase is that the velocity of autonomous class vehicles is still greater than or equal to the free-flow velocity of human-driven vehicles. The optimal space fraction of HDVs and AVs in semi-congested phase is determined as:

$$\alpha_{sc,i,\mathrm{A}} = \frac{k_{i,\mathrm{A}}}{k^*_{\mathrm{c,A}}}, \quad \alpha_{sc,i,\mathrm{H}} = \frac{k_{i,\mathrm{H}}}{k_{\mathrm{c,H}}} \tag{2}$$

where $k^*_{\mathrm{c,A}}$ is the "perceived" critical density of autonomous vehicles and is defined as:

$$k^*_{\mathrm{c,A}} = k_{\mathrm{c,A}} \left[-a_{\mathrm{m,A}} \ln \left(\frac{v_{\mathrm{f,H}}}{v_{\mathrm{f,A}}} \right) + 1 \right]^{\frac{1}{a_{\mathrm{m,A}}}} \tag{3}$$

where $v_{\mathrm{f,A}}$ and $v_{\mathrm{f,H}}$ are the free-flow velocities for AVs and HDVs accordingly. Also $a_{\mathrm{m,A}}$ is a state varying model parameter. *Congested Phase*: Both human-driven and autonomous vehicles drive at lower speed than the free-flow velocity. In congested phase, autonomous and human-driven class vehicles both have the same velocity. The space fraction of HDVs and AVs in congested phase is determined as follow:

$$\begin{aligned} \alpha_{c,i,\mathrm{A}} &= \frac{A}{B}, \quad \alpha_{c,i,\mathrm{H}} + \alpha_{c,i,\mathrm{A}} = 1 \\ A &= \Big((k_{\mathrm{c,H}} - k_{\mathrm{J,H}}) k_{\mathrm{c,A}} v_{\mathrm{f,A}} \\ &\quad - (k_{\mathrm{c,A}} - k_{\mathrm{J,A}}) k_{\mathrm{c,H}} v_{\mathrm{f,H}} \Big) k_{\mathrm{A}} k_{\mathrm{H}} \\ &\quad + (k_{\mathrm{c,A}} - k_{\mathrm{J,A}}) k_{\mathrm{c,H}} k_{\mathrm{J,H}} v_{\mathrm{f,H}}\ k_{\mathrm{A}} \\ B &= (k_{\mathrm{c,A}} - k_{\mathrm{J,A}}) k_{\mathrm{c,H}} k_{\mathrm{J,H}} v_{\mathrm{f,H}} k_{\mathrm{A}} \\ &\quad + (k_{\mathrm{c,H}} - k_{\mathrm{J,H}}) k_{\mathrm{c,A}} k_{\mathrm{J,A}} v_{\mathrm{f,A}} k_{\mathrm{H}} \end{aligned} \tag{4}$$

where $k_{\mathrm{J,H}}$ is the jam density for the human-driven vehicles and $k_{\mathrm{J,A}}$ is the jam density for the autonomous vehicles. The total average flow relationship in a Macroscopic Fundamental Diagram (MFD) can be calculated through following equation:

$$Q_i = k_{i,\mathrm{H}} V\Big(\frac{k_{i,\mathrm{H}}}{\alpha_{i,\mathrm{H}}}\Big) + k_{i,\mathrm{A}} V\Big(\frac{k_{i,\mathrm{A}}}{\alpha_{i,\mathrm{A}}}\Big) \tag{5}$$

where Q_i is the total average flow which depends on the densities and velocities of both human-driven vehicles and autonomous vehicles, $V\left(\frac{k_{i,\mathrm{H}}}{\alpha_{i,\mathrm{H}}}\right)$ is the suggested velocity for HDVs and $V\left(\frac{k_{i,\mathrm{A}}}{\alpha_{i,\mathrm{A}}}\right)$ is the suggested velocity for AVs.

2.2 Equations of Motion

Consider a non-signalized heterogeneous traffic network. For a cell $i \in \{1, \cdots, n\}$, let $q_{i,\mathrm{A}}$ and $q_{i,\mathrm{H}}$ be outflow (number of AVs and HDVs leaving the cell i to the adjacent cell $i+1$) and d_i be the uncontrolled traffic demand including the off-ramps and on-ramps traffic flows. Also, consider ℓ as the length of the segment and γ as the number of the lanes in the segment. Then, the density of cell i (for each type of vehicle) is updated according

to the conservation of vehicles law (Boriboonsomsin et al. (2012)). Specifically,

$$k_{i,\mathrm{A}}(t+1) = k_{i,\mathrm{A}}(t) + \frac{T}{\ell_i \gamma_i}(q_{i-1,\mathrm{A}}(t) - q_{i,\mathrm{A}}(t) + d_{i,\mathrm{A}}(t)) \tag{6a}$$

$$k_{i,\mathrm{H}}(t+1) = k_{i,\mathrm{H}}(t) + \frac{T}{\ell_i \gamma_i}(q_{i-1,\mathrm{H}}(t) - q_{i,\mathrm{H}}(t) + d_{i,\mathrm{H}}(t)) \tag{6b}$$

which $q_{i,\mathrm{H}}(t) = k_{i,\mathrm{H}}(t).v_{i,\mathrm{H}}(t)$ and $q_{i,\mathrm{A}}(t) = k_{i,\mathrm{A}}(t).v_{i,\mathrm{A}}(t)$.

Following the heterogeneous METANET model, the velocity of each class of vehicles can be described as

$$v_{i,\mathrm{A}}(t+1) = v_{i,\mathrm{A}}(t) + \frac{T}{\ell}\Big[v_{i,\mathrm{A}}(t)\Big(v_{i-1,\mathrm{A}}(t) - v_{i,\mathrm{A}}(t)\Big) - \frac{\gamma_{\mathrm{A}}}{\tau_{\mathrm{A}}}\frac{k_{i+1,\mathrm{A}}(t) - k_{i,\mathrm{A}}(t)}{k_{i,\mathrm{A}}(t) + k_{\mathrm{c,A}}\zeta_{\mathrm{A}}}\Big] + \frac{T}{\tau}\Big(U_{i,\mathrm{A}}(t) - v_{i,\mathrm{A}}(t)\Big) \tag{7a}$$

$$v_{i,\mathrm{H}}(t+1) = v_{i,\mathrm{H}}(t) + \frac{T}{\ell}\Big[v_{i,\mathrm{H}}(t)\Big(v_{i-1,\mathrm{H}}(t) - v_{i,\mathrm{H}}(t)\Big) - \frac{\gamma_{\mathrm{H}}}{\tau}\frac{k_{i+1,\mathrm{H}}(t) - k_{i,\mathrm{H}}(t)}{k_{i,\mathrm{H}}(t) + k_{\mathrm{c,H}}\zeta_{\mathrm{H}}}\Big] + \frac{T}{\tau_{\mathrm{H}}}\Big(U_{i,\mathrm{H}}(t) - v_{i,\mathrm{H}}(t)\Big) \tag{7b}$$

with

$$U_{i,\mathrm{A}} = (\beta_{i,\mathrm{A}})v_{\mathrm{f,A}}\exp\left[\frac{-1}{a_{\mathrm{m,A}}}\left(\frac{k_{i,\mathrm{A}}(t)}{\alpha_{i,\mathrm{A}}k_{\mathrm{c,A}}}\right)^{a_{\mathrm{m,A}}}\right] \tag{8a}$$

$$U_{i,\mathrm{H}} = (\beta_{i,\mathrm{H}})v_{\mathrm{f,H}}\exp\left[\frac{-1}{a_{\mathrm{m,H}}}\left(\frac{k_{i,\mathrm{H}}(t)}{\alpha_{i,\mathrm{H}}k_{\mathrm{c,H}}}\right)^{a_{\mathrm{m,H}}}\right] \tag{8b}$$

where $a_{m,\mathrm{H}}$ and $a_{m,\mathrm{A}}$ are state varying model parameters that are a function of the density of each vehicle class. ζ_{H}, ζ_{A}, τ_{A} and τ_{H} are model parameters for human and autonomous vehicles. In addition, $\beta_{i,\mathrm{A}}$ and $\beta_{i,\mathrm{H}}$ are considered as the control commands adjusting the suggested velocity to the autonomous vehicles and human-driven vehicles. $\beta_{i,\ rmA} = 1$ or $\beta_{i,\mathrm{H}} = 1$ means that the controller is following the velocity-density steady state behavior for that specific vehicle type. Also, $\beta_{i,\mathrm{A}} = 0$ or $\beta_{i,\mathrm{H}} = 0$ means that the controller is commanding the vehicles of each class to stop or to drive with the constrained minimum speed on the road. It is assumed that the AVs are connected to the infrastructure so they can receive the control commands directly and HDVs can receive the suggested velocities through the Variable Speed Limit (VSL) signs on the road. It is important to note that, the control command for HDVs is considered $\beta_{i,\mathrm{H}} = 1$ for the rest of the paper. The terms $\alpha_{i,\mathrm{A}}$ and $\alpha_{i,\mathrm{H}}$ in Eqs. (8a, 8b), are the coupling terms in which relates the dynamics of HDVs to AVs in the METANET model.

For a traffic network consisting of n cell, by combining equations (6a)-(8b), the equations of motion can be expressed as

$$\dot{x} = \mathcal{F}(x) + \mathcal{G}(x)u + d \tag{9}$$

where $x = [x_1, \cdots, x_{4n}]^{\mathrm{T}}$, $d = [d_1, \cdots, d_{4n}]^{\mathrm{T}}$, $u = [\beta_{1,\mathrm{A}}, \beta_{1,\mathrm{H}}, \cdots, \beta_{n,\mathrm{A}}, \beta_{n,\mathrm{H}}]$, $\mathcal{F} = [f_1, \cdots, f_{4n}]^{\mathrm{T}}$, $\mathcal{G} = [g_1, \cdots, g_{2n}]^{\mathrm{T}}$. For $i \in \{1, \cdots, n\}$ $g_i = [0]_{2n\times 2n}$, For $i \in \{n, \cdots, 2n\}$, $g_i = \Bigg[v_{\mathrm{f,A}}\exp\left[\frac{-1}{a_{\mathrm{m,A}}}\left(\frac{k_{i,\mathrm{A}}(t)}{\alpha_{i,\mathrm{A}}k_{\mathrm{c,A}}}\right)^{a_{\mathrm{m,A}}}\right]$ $, v_{\mathrm{f,H}}\exp\left[\frac{-1}{a_{\mathrm{m,H}}}\left(\frac{k_{i,\mathrm{H}}(t)}{\alpha_{i,\mathrm{H}}k_{\mathrm{c,H}}}\right)^{a_{\mathrm{m,H}}}\right]\Bigg]$

3 Traffic Management Controller

This section focuses on the design of a hierarchical macroscopic traffic management controller to improve the performance of a heterogeneous traffic network in terms of mobility. The controller has a two-level structure with a decentralized ES algorithm in the upper-level and filtered feedback linearization in the lower-level. The description of these algorithms are given below.

3.1 Higher-level Controller: Decentralized Extremum Seeking Controller

ES control approach is a real-time control technique that optimize the steady-state behaviour of an unknown system which is done by estimating the gradients of the input-output mapping. As it is shown in Fig. 1, the higher level controller contains a gradient estimator and an optimizer block. The extremum seeking block gets the cost function value J_i and the constraint vector $y_{c,i}$ from the plant and then estimates the gradient of system's outputs. The optimizer block, takes the gradient estimator outputs along with the constraint vector from the traffic network and finally estimates the inputs of the lower-level controller which are $k^*_{i,\mathrm{H}}$ and $k^*_{i,\mathrm{A}}$. For each cell $i \in \{1, \cdots, n\}$, we consider the cost function to average flow expresses in Eq. (5). In particular,

$$\max_{k_{i,\mathrm{H}}, k_{i,\mathrm{A}}} J_i(t) = Q_i \tag{10}$$

subjected to the dynamics equations (6)-(8).

To solve the optimization problem in Eq.(10), we develop a decentralized ES control framework. ES controller is a real-time optimizer and its main advantage is that it is model-free (Zotos et al. (1997),Straus et al. (2019a)) . This enables the ES control to control a complex dynamic system and find the optimal operating states of the heterogeneous traffic network. The details of these controllers are described below. In the ES control problems, J, which is a function of time, is actually the output of a complex dynamic model. The whole control schematic of the traffic system described in (Ariyur and Krstic (2003)). To determine the optimal control command $\beta_{i,\mathrm{A}}$ and $\beta_{i,\mathrm{H}}$ in each cell, the calculated J_i and defined set of constraints $y_{c,i}$ passes through a HP (High-Pass) filter $\mathcal{F}_{i,\mathrm{HF}} = \frac{s}{s+\omega_{i,\mathrm{H}}}$, where $\omega_{i,\mathrm{H}}$ is the frequency for the high-pass filter. The high-pass filter's output is multiplied by the sinusoidal signal with the same perturbation frequency, $A_i \sin(\Omega t - \phi_i)$, where ϕ_i is the phase lag. Then, the output signal goes through a LP (Low-Pass) filter to show us the direction of maximizing the cost function and tracing the boundary.

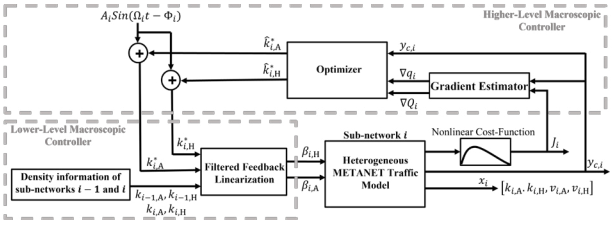

Fig. 1. Schematic of the whole system consisting the MIMO plant, Extremum Seeking, Optimizer and Filtered Feedback Linearization

Boundary tracing in the optimizer block is conducted when any boundary constraint is passed and it is active, otherwise, the problem is like an unconstrained problem. In particular, the gradient of the static map ∇Q dominates when no constraint is active, on the other hand, when we have an active constraint in the system, the optimiser updates the lower-level input signals based on the constraint boundary gradient ∇g. The required conditions and equations of optimiser block are addressed in (Liao et al. (2019)).

To ensure the proposed controller's stability and convergence, a set of conditions needs to be met (Straus et al. (2019b)). It follows from the cost function (10) and the form of the FD function expressed in Eq. (5) that the first and second derivatives of the cost function J_i with respect to $k_{i,\mathrm{A}}$ and $k_{i,\mathrm{H}}$ should exist. Additionally, it can be shown that there exist $k^*_{i,\mathrm{A}}$ and $k^*_{i,\mathrm{H}}$ such that the first derivative of $J_i'(k^*_{i,kA}) = 0$, $J_i'(k^*_{i,kH}) = 0$ and $J^{''}(k^*_{i,\mathrm{A}}) \leq 0$, $J^{''}(k^*_{i,\mathrm{H}}) \leq 0$. Furthermore, we select the high-pass filter's cut-off frequencies $\omega_{i,\mathrm{H}}$ to be lower than the frequency of the perturbation signal Ω_i. In particular, in this paper, we select $\omega_{i,\mathrm{H}}$ to be 5 times lower than Ω_i (i.e., $\omega_{i,\mathrm{H}} \leq 0.1\Omega_i$). By satisfying these conditions, the ES converges to its optimal state $k^*_{i,\mathrm{H}}, k^*_{i,\mathrm{A}}$ (Straus et al. (2019b)).

3.2 Lower-level Controller: Filtered Feedback Linearization (FFL)

The high level controllers' outputs estimate the optimal density k^*_{A} and k^*_{H} of each cell which will then be fed to a lower-level control as a reference signal. In the lower-level control, we employ a filtered feedback linearization approach to determine the required control command $\beta_{i,\mathrm{A}}$ and $\beta_{i,\mathrm{H}}$. We select filtered feedback linearization controller in the lower-level since this controller only needs limited information from the dynamic traffic model, specifically, the system's relative degree and an estimate of the nonlinear extension of the high-frequency-gain matrix, and does not require any knowledge of the disturbance in the system (Hoagg and Seigler (2013, 2015); Ghasemi (2017); Ghasemi et al. (2018)). Furthermore, it can be shown that FFL is capable of the $\mathcal{L}_\infty$ of the command following error arbitrarily small regardless of the presence of undetermined disturbances in the system (Ghasemi et al. (2018)). Below, we summarize the FFL control approach.

Considering $\mathcal{Y}_i = [k_{i,\mathrm{A}}, k_{i,\mathrm{H}}]^{\mathrm{T}}$, evaluating the second derivative of $\mathcal{Y}$ yields

$$\begin{bmatrix} \ddot{k}_{i,\mathrm{A}} \\ \ddot{k}_{i,\mathrm{H}} \end{bmatrix} = \begin{bmatrix} \Psi_{i,\mathrm{A}}(x,\phi_d) \\ \Psi_{i,\mathrm{H}}(x,\phi_d) \end{bmatrix} + \Gamma_i(x_i) \begin{bmatrix} \beta_{i,\mathrm{A}} \\ \beta_{i,\mathrm{H}} \end{bmatrix} \tag{11}$$

where $\Gamma_i(x_i)$ is non-singular for $k_{i,\mathrm{A}} \in (0, k_{\mathrm{J,A}})$, $k_{i,\mathrm{H}} \in (0, k_{\mathrm{J,H}})$, $v_{i,\mathrm{A}} \in (0, v_{\mathrm{f,A}})$, $v_{i,\mathrm{H}} \in (0, v_{\mathrm{f,H}})$ and $\phi_d = [d, \dot{d}, \ddot{d}]^{\mathrm{T}}$.

Then, the control commands generated by the standard feedback linearization approach can be expressed as

$$\begin{bmatrix} \beta^*_{i,\mathrm{A}} \\ \\ \beta^*_{i,\mathrm{H}} \end{bmatrix} = -\Gamma_i^{-1}(X) \begin{bmatrix} \nu_{i,\mathrm{A}} + \Psi_{i,\mathrm{A}} \\ \nu_{i,\mathrm{H}} + \Psi_{i,\mathrm{H}} \end{bmatrix} \tag{12}$$

$$\nu_{i,\mathrm{A}} = \ddot{k}^*_{i,\mathrm{A}} + a_{i,1}(\dot{k}^*_{i,\mathrm{A}} - \dot{k}_{i,\mathrm{A}}) + a_{i,0}(k^*_{i,\mathrm{A}} - k_{i,\mathrm{A}}) \tag{13a}$$

$$\nu_{i,\mathrm{H}} = \ddot{k}^*_{i,\mathrm{H}} + a_{i,1}(\dot{k}^*_{i,\mathrm{H}} - \dot{k}_{i,\mathrm{H}}) + a_{i,0}(k^*_{i,\mathrm{H}} - k_{i,\mathrm{H}}) \tag{13b}$$

where $a_{i,0}$ and $a_{i,1}$ are constants. It follows from Eq. (12) that $\beta^*_{i,\mathrm{A}}, \beta^*_{i,\mathrm{H}}$ require the measurement of the disturbance d as well as knowledge of $\Psi_i(x, \phi_d)$ which may not be feasible in practice.

To this end, we determine the implementable control commands $\beta_{i,\mathrm{A}}, \beta_{i,\mathrm{H}}$ by passing $\beta^*_{i,\mathrm{A}}, \beta^*_{i,\mathrm{H}}$ through a low-pass filter. Specifically, let $\beta_{i,\mathrm{A}}, \beta_{i,\mathrm{H}}$ satisfy

$$\eta_z(\mathbf{p})\beta_{i,\mathrm{A}} = \eta_z(0)\beta^*_{i,\mathrm{A}} \tag{14}$$

$$\eta_z(\mathbf{p})\beta_{i,\mathrm{H}} = \eta_z(0)\beta^*_{i,\mathrm{H}} \tag{15}$$

where $\mathbf{p} = d/dt$, and η_z is a real polynomial of order $\rho \geq 1$ whose coefficients depend on the real parameter $z > 0$. The required conditions and examples of $\eta_z(s)$ are addressed in (Hoagg and Seigler (2013)). For example, $\eta_z(s)$ can be a polynomial $\eta_z(s) = (s+z)^3$.

Substituting Eq. (11) into Eq. (12) and substituting this result into Eqs. (15)-(15), FFL controller is defined as

$$\begin{bmatrix} (\eta_z(\mathbf{p}) - \eta_z(0))\beta_{i,\mathrm{A}} \\ (\eta_z(\mathbf{p}) - \eta_z(0))\beta_{i,\mathrm{H}} \end{bmatrix} = \eta_z(0)\Gamma_i^{-1}(U_{i-1}, U_i, k_{i-1}, k_i)_{\mathrm{A,H}} \begin{bmatrix} \ddot{e}_{i,\mathrm{A}} + a_1\dot{e}_{i,\mathrm{A}} + a_0 e_{i,\mathrm{A}} \\ \ddot{e}_{i,\mathrm{H}} + a_1\dot{e}_{i,\mathrm{H}} + a_0 e_{i,\mathrm{H}} \end{bmatrix} \tag{16a}$$

where $e_{i,\mathrm{A}} = k^*_{i,\mathrm{A}} - k_{i,\mathrm{A}}$ and $e_{i,\mathrm{H}} = k^*_{i,\mathrm{H}} - k_{i,\mathrm{H}}$ and $0 \leq \beta_{i,\mathrm{A}}, \beta_{i,\mathrm{H}} \leq 1$

The controllers (12) and (16) are mathematically equivalent. However, unlike Eq. (12), the control (16) does not require measurement of d_i or Ψ_i. Properties of the lower-level closed-loop are addressed by (Hoagg and Seigler (2013))-Lemma 1. Specifically, it is shown that there exists $z_{\mathrm{s}} > z_0$ such that for $z > z_{\mathrm{s}}$, the control command given by Eq. (16) stabilizes the dynamic system and makes the tracking error arbitrarily small.

4 Simulation and Results

In this section, we present a case study to demonstrate the effectiveness of the proposed approach for improving the mobility of a heterogeneous traffic network. We compare the outcomes of the proposed control approach with a scenario where there is no controller and vehicles are following the classic METANET model dynamics. In this study, we considered a real-world network with 10 heterogeneous cells consisting HDVs and AVs. We used the I-485 N of Exit 28 (Mallard Creek Rd, Mecklenburg County, NC in Fig. 2) traffic flow data which was reported in Tuesday 22 December 2020 to calibrate the HDVs' model parameters and model the origin outflow in our simulation. The concentration is on eastbound PM peak hour of the highway which is between 4:30-5:30 PM. For both scenarios (with no-controller and with ES-FFL controller), the boundary cells which set the demand and supply of the whole traffic system and the initial states are the same. I-485 inner highway has 4 lanes with the speed limit of 70 mph for HDVs.

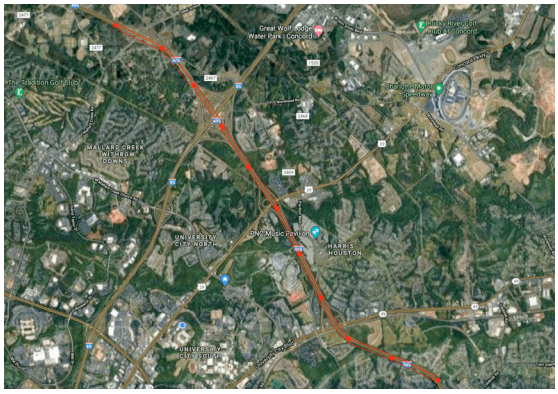

Fig. 2. I-485 inner highway between Mallard Creek Rd and Caldwell Rd, Charlotte, North Carolina

4.0.1 Heterogeneous Network The focus of this section is only on one of the cells (cell 3) that is already in the congested phase and it is experiencing a congestion delay. Initially, the target cell has $k_{3,\mathrm{A}} = 77, k_{3,\mathrm{H}} = 18\frac{veh}{mile.lane}$ and both types of vehicles have same velocity of $v_{3,\mathrm{A}} = v_{3,\mathrm{H}} = 47mph$. The HDVs model parameters that were calibrated based on the NCDOT traffic flow data and the AVs' model parameters that were predicted by simulating the same traffic scenario in PTV VISSIM traffic simulator using CoExist AV models are listed here; $a_{m,\mathrm{A}} = h(k_{i,\mathrm{A}}), a_{m,\mathrm{H}} = h(k_{i,\mathrm{H}})$, $\gamma_{\mathrm{A}} = 44, \gamma_{\mathrm{H}} = 60\frac{mile^2}{h}$, $\eta_{\mathrm{A}} = 14, \eta_{\mathrm{H}} = 10\frac{veh}{mile.h}$, $\tau_{\mathrm{A}} = 3, \tau_{\mathrm{H}} = 12s$. The length of each cell is considered as $\ell = 1$ mile and there are 4 lanes $\gamma = 4$ in each cell. Finally, the variables' values for each controller (ES and FFL) is listed here: $A_i = 1$, $\Omega = 0.02\pi\frac{rad}{s}$, $\omega_{i,\mathrm{H}} = 0.2\Omega_i$, $\omega_{i,\mathrm{L}} = 0.1\omega_{i,\mathrm{H}}$, $z = 100$, $a_{i,1} = 20$ and, $a_{i,0} = 1$.

Here, the goal is to maximize the average flow rate of the target cell and improve its mobility. Based on the NCDOT traffic data report, the HDVs' density in cell 3 varies between 16 to $21\frac{veh}{mile.lane}$ as it is shown in Fig.3 (second row). The higher level macro controller (ES) estimates the optimum density of AVs in cell 3 ($k^*_{3,\mathrm{A}}$) according to the density of HDVs and the defined cost function in Eq.(10). The estimated AV's density is fed into the lower-level macro controller (FFL) as the reference trajectory (desired density). And FFL generates the controller command in cells 2 and 3 ($\beta_{2,\mathrm{A}}, \beta_{3,\mathrm{A}}$) to control the suggested velocity of AVs in two adjacent cells (Upstream cell and the target cell).

As it is shown in Fig.3, in the first row, the density of autonomous vehicles in the "ES-FFL Controller" scenario is less than the "No Controller" scenario. The density of HDVs in both scenarios is exactly same. By looking at the cost function values in Fig. 3, it can be seen that the hierarchical controller design is effectively improving the mobility of the target cell and maximizing the defined cost function in comparison to the scenario where there is not any active controller in the traffic system. In addition, since the the optimum density of AVs in cell 3 is feasible, the constraints on the density are not active and so they do not have any effect on the optimum solution. In the "ES-FFL Controller" scenario, the estimated desired density for AVs in cell 3 ($k^*_{3,\mathrm{A}}$) is the reference trajectory of the density of AVs. Filtered Feedback Linearization controller

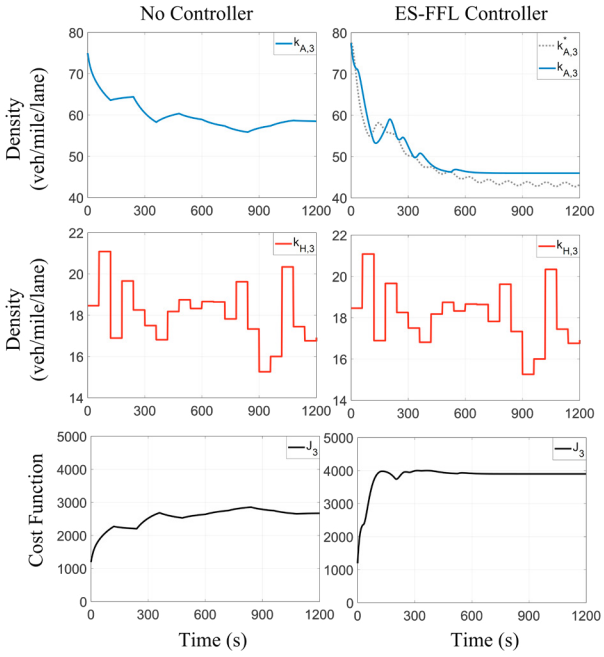

Fig. 3. Density of AVs (first row), density of HDVs (second row) and, the cost-function value (third row) for both "No Controller" scenario (first column) and the "ES-FFL Controller" scenario (second column) for the target cell (cell 3) is shown in this figure.The desired density of cell 3 for AVs ($k^*_{A,3}$) which is estimated by the ES controller is also shown by a "dashed" line.

gets the AVs' reference density in each time step and calculates the desired controller commands for the target cell and its upstream cell as it is shown in Fig. 4.

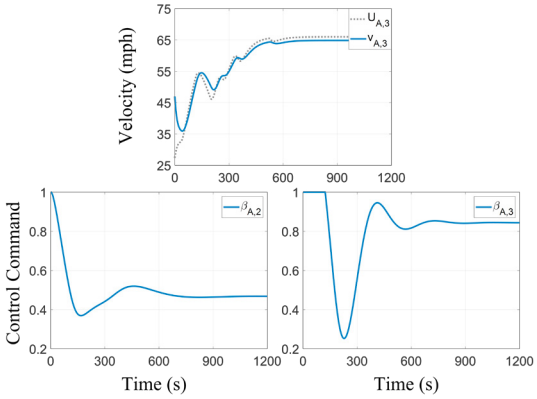

Fig. 4. Suggested velocity ($U_{A,3}$) and velocity ($v_{A,3}$) of autonomous vehicles in cell 3 (first row) is shown in this figure. The controller commands generated for cells 2 and 3 (second row) are also shown here.

In Fig. 4, the velocity of AVs in the target cell is following the suggested velocity with small errors. The reason that there are some differences between the suggested velocity and the actual average velocity of AVs is that the average velocity equation (Eq.7a) contains two other terms which may reduce the effect of the suggested velocity term. Since the ultimate goal is to reduce the density of the target cell, the FFL controller reduces the inflow of the target cell by lowering the suggested velocity of its upstream cell. Also,

it increases the outflow of the target cell by increasing the suggested velocity of cell 3. As it was stated in section 2.2, the control commands for HDVs are considered to be ($\beta_{2,\mathrm{H}} = \beta_{3,\mathrm{H}} = 1$ which means that the controller is not controlling the velocity of HDVs directly.

5 Conclusions

This paper focuses on modeling and controlling a non-signalized heterogeneous freeway traffic network consisting of Human-Driven Vehicles (HDVs) and Autonomous Vehicles (AVs). In this paper, the heterogeneity in the operational characteristics and controllability of each type of vehicle is considered. It is assumed that autonomous vehicles have a higher free-flow velocity and model parameters compared to human-driven vehicles. We developed a two-level control structure to improve mobility in the traffic network. At the higher level, a decentralized ES control approach is designed to determine an optimal density of HDVs and/or AVs so that the average flow within a cell is maximized. At the lower level, a filtered feedback linearization control approach is designed to determine the suggested velocity of both autonomous vehicles and human-driven vehicles such that the density of the AVs and HDVs reaches the values set by the upper-level controller. In the future, we consider to what extend the mobility of the traffic network can be improved if only autonomous vehicles can receive the velocity commands set by the higher-level controller. We further plan to validate our control approach with more sophisticated traffic simulators.

References

Ariyur, K.B. and Krstic, M. (2003). *Real-time optimization by extremum-seeking control*. John Wiley & Sons.

Benzoni-Gavage, S. and Colombo, R.M. (2003). An-populations model for traffic flow. *European Journal of Applied Mathematics*, 14(5), 587–612.

Boriboonsomsin, K., Barth, M.J., Zhu, W., and Vu, A. (2012). Eco-routing navigation system based on multisource historical and real-time traffic information. *IEEE Transactions on Intelligent Transportation Systems*, 13(4), 1694–1704.

Chanut, S. and Buisson, C. (2003). Macroscopic model and its numerical solution for two-flow mixed traffic with different speeds and lengths. *Transportation research record*, 1852(1), 209–219.

Cookson, G. and Pishue, B. (2017). Inrix global traffic scorecard–appendices. *INRIX research*.

DeHaan, D. and Guay, M. (2005). Extremum-seeking control of state-constrained nonlinear systems. *Automatica*, 41(9), 1567–1574.

Ghasemi, A.H. (2017). Slewing and vibration control of a single-link flexible manipulator using filtered feedback linearization. *Journal of Intelligent Material Systems and Structures*, 28(20), 2887–2895.

Ghasemi, A.H., Hoagg, J.B., and Seigler, T. (2018). Decentralized filtered feedback linearization for uncertain nonlinear systems. *International Journal of Robust and Nonlinear Control*, 28(4), 1496–1506.

Hoagg, J.B. and Seigler, T. (2013). Filtered-dynamic-inversion control for unknown minimum-phase systems with unknown-and-unmeasured disturbances. *International Journal of Control*, 86(3), 449–468.

Hoagg, J.B. and Seigler, T. (2015). Decentralized filtered dynamic inversion for uncertain minimum-phase systems. *Automatica*, 61, 192–200.

Lazar, D.A., Pedarsani, R., Chandrasekher, K., and Sadigh, D. (2018). Maximizing road capacity using cars that influence people. In *2018 IEEE Conference on Decision and Control (CDC)*, 1801–1808. IEEE.

Liao, C.K., Manzie, C., Chapman, A., and Alpcan, T. (2019). Constrained extremum seeking of a mimo dynamic system. *Automatica*, 108, 108496.

Liu, S., De Schutter, B., and Hellendoorn, H. (2014). Model predictive traffic control based on a new multiclass metanet model. *IFAC Proceedings Volumes*, 47(3), 8781–8786.

Logghe, S. (2003). Dynamic modeling of heterogeneous vehicular traffic. *Faculty of Applied Science, Katholieke Universiteit Leuven, Leuven*, 2.

Papageorgiou, M. (1983). *Applications of automatic control concepts to traffic flow modeling and control*. Springer.

Ross, C. and Guhathakurta, S. (2017). Autonomous vehicles and energy impacts: a scenario analysis. *Energy Procedia*, 143, 47–52.

Shahri, P.K. and Ghasemi, A.H. (2022). Heterogeneous traffic management using metanet model with filtered feedback linearization control approach. Technical report, SAE Technical Paper.

Shahri, P.K., Ghasemi, A.H., and Izadi, V. (2020). Optimal lane management in heterogeneous traffic network using extremum seeking approach. Technical report, SAE Technical Paper.

Sharon, G. and Stone, P. (2017). A protocol for mixed autonomous and human-operated vehicles at intersections. In *International Conference on Autonomous Agents and Multiagent Systems*, 151–167. Springer.

Straus, J., Krishnamoorthy, D., and Skogestad, S. (2019a). On combining self-optimizing control and extremum-seeking control–applied to an ammonia reactor case study. *Journal of Process Control*, 78, 78–87.

Straus, J., Krishnamoorthy, D., and Skogestad, S. (2019b). On combining self-optimizing control and extremum-seeking control–applied to an ammonia reactor case study. *Journal of Process Control*, 78, 78–87.

Wang, J., Peeta, S., and He, X. (2019). Multiclass traffic assignment model for mixed traffic flow of human-driven vehicles and connected and autonomous vehicles. *Transportation Research Part B: Methodological*, 126, 139–168.

Ye, L. and Yamamoto, T. (2018). Modeling connected and autonomous vehicles in heterogeneous traffic flow. *Physica A: Statistical Mechanics and its Applications*, 490, 269–277.

Zheng, F., Liu, C., Liu, X., Jabari, S.E., and Lu, L. (2020). Analyzing the impact of automated vehicles on uncertainty and stability of the mixed traffic flow. *Transportation research part C: emerging technologies*, 112, 203–219.

Zotos, X., Naef, F., and Prelovsek, P. (1997). Transport and conservation laws. *Physical Review B*, 55(17), 11029.